

1 *Supplement of*  
2 **Importance of ice elasticity in simulating tide-induced grounding line variations**  
3 **along prograde bed slopes**

4 Natalya Maslennikova et al.

5 *Correspondence to:* Natalya Maslennikova ([nmaslenn@cougarnet.uh.edu](mailto:nmaslenn@cougarnet.uh.edu))

6 The copyright of individual parts of the supplement might differ from the article license.

7 **S.1. Reference measurements**

8 Grounding zone measurements were performed using pairs of DInSAR interferograms at high and low tide; bedrock  
 9 slope and ice thickness were calculated using Bed Machine Antarctica, and ice flow speed was determined using  
 10 MEaSURES (version 2). The measurements, performed along ~20 km-long flow lines (see Figure 1), are provided in  
 11 Table S1.

12 **Table S1.** Grounding zone (GZ), ice thicknesses, bed slope, and ice flow speed measurements over Totten (TOT),  
 13 Moscow University (MU), and Rennick (REN) glaciers.

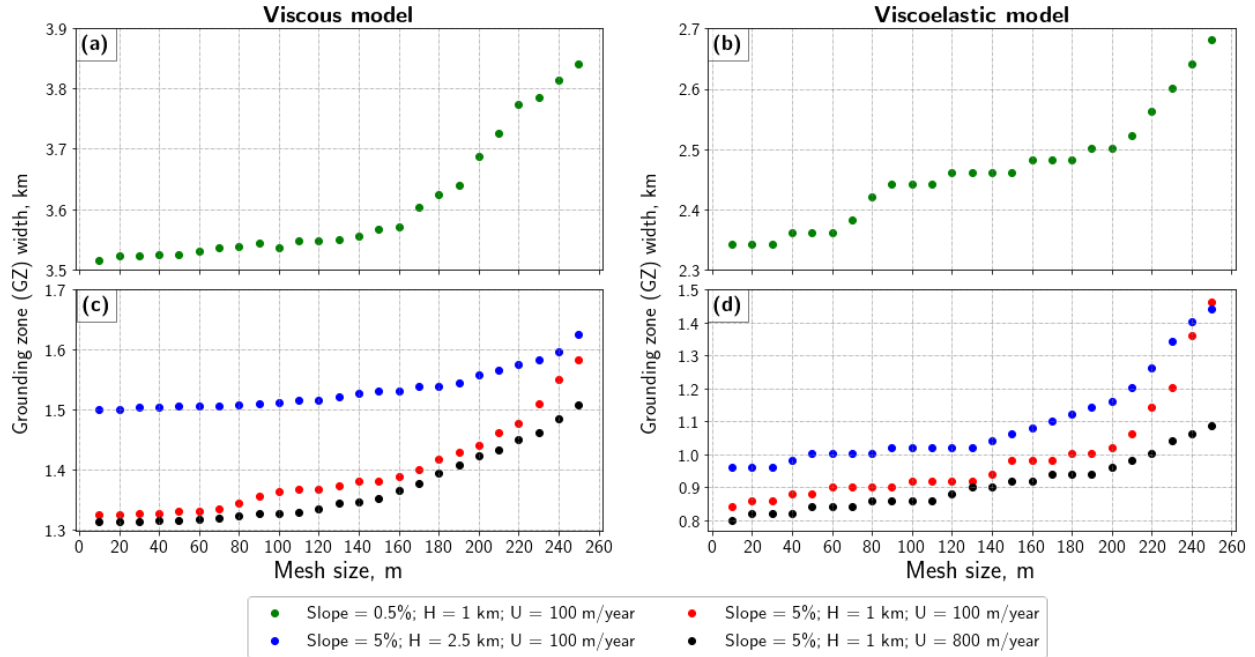
Glacier	Flow line	GZ, km	Bed slope $\alpha$ , %	Ice thickness $H$ , km	Ice flow speed $v$ , m/yr	Profile type
MU	0	0.6	5.0	1.8	322	Main
MU	1	1.3	2.8	1.8	319	Main
MU	2	1.6	2.4	1.8	316	Main
MU	3	1.7	2.0	1.7	301	Main
MU	4	1.6	2.8	1.7	291	Main
MU	5	1.6	2.9	1.7	291	Main
MU	6	1.4	2.5	1.7	291	Main
MU	7	1.6	2.2	1.7	301	Main
MU	8	1.6	2.1	1.7	310	Main
MU	9	1.4	2.7	1.7	317	Main
MU	10	0.8	5.0	1.8	325	Main
MU	11	0.9	4.9	1.8	327	Main
MU	12	1.0	4.9	1.8	334	Main
MU	13	1.3	3.3	1.9	339	Main
MU	14	1.7	1.7	1.9	348	Main
MU	15	1.8	1.6	1.9	361	Main
MU	16	2.2	1.0	2.0	369	Main
MU	17	1.9	1.7	2.1	369	Main
MU	18	1.7	1.5	2.2	372	Main
MU	19	1.6	2.3	2.2	378	Main
MU	20	1.8	1.4	2.3	373	Main
MU	21	1.9	1.5	2.4	373	Main
MU	22	2.0	1.5	2.4	354	Main
MU	23	1.9	1.7	2.4	347	Main
MU	24	1.4	3.1	2.4	342	Main
MU	25	0.7	4.5	2.4	327	Main
MU	26	0.4	4.9	2.4	319	Main
MU	27	0.4	5.4	2.4	307	Extra
MU	28	0.5	5.4	2.3	289	Extra
MU	29	1.1	3.9	2.3	294	Main
MU	30	5.0	0.01	2.4	327	Main
MU	31	5.2	0.02	2.3	314	Main
MU	32	3.9	0.4	2.3	292	Main
MU	33	3.3	0.3	2.2	261	Main
MU	34	3.3	0.3	2.2	243	Main
MU	35	3.4	0.3	2.2	228	Main
MU	36	3.6	0.4	2.2	207	Main
MU	37	3.7	0.3	2.2	185	Main
MU	38	3.8	0.3	2.1	168	Main
MU	39	9.0	0.1	2.1	165	Main
MU	40	10.2	0.1	2.0	158	Main

MU	41	11.5	0.1	1.9	151	Main
MU	42	11.8	0.1	1.8	155	Main
MU	43	12.5	0.01	1.7	149	Main
REN	0	0.8	5.2	0.7	113	Extra
REN	1	1.4	2.4	0.8	135	Extra
REN	2	1.9	1.5	0.9	150	Extra
REN	3	2.1	1.2	0.9	158	Extra
REN	4	2.2	1.2	1.0	171	Main
REN	5	2.4	1.0	1.0	176	Main
REN	6	2.4	0.8	1.0	183	Main
REN	7	2.9	0.6	1.0	186	Main
REN	8	2.8	0.7	1.1	187	Main
REN	9	3.1	0.6	1.1	188	Main
REN	10	2.8	0.7	1.1	187	Main
REN	11	3.3	0.3	1.1	187	Main
REN	12	3.2	0.5	1.2	185	Main
REN	13	2.8	0.5	1.1	183	Main
REN	14	2.3	1.0	1.2	178	Main
REN	15	1.8	1.5	1.1	174	Main
REN	16	1.9	1.1	1.1	169	Main
REN	17	2.2	1.0	1.0	162	Main
REN	18	2.2	1.1	1.0	152	Main
TOT	0	0.9	4.6	2.3	696	Main
TOT	1	1.0	4.1	2.3	674	Main
TOT	2	1.8	2.1	2.4	722	Main
TOT	3	3.5	0.4	2.4	754	Main
TOT	4	4.6	0.2	2.3	758	Main
TOT	5	6.3	0.06	2.3	740	Main
TOT	6	7.0	0.03	2.3	731	Main
TOT	7	7.5	0.06	2.2	709	Main
TOT	8	7.6	0.07	2.2	690	Main
TOT	9	6.0	0.03	2.1	680	Main
TOT	10	5.5	0.02	2.1	683	Main
TOT	11	5.6	0.1	2.0	735	Main
TOT	12	3.0	0.5	1.9	747	Main
TOT	13	2.2	1.0	1.9	683	Main
TOT	14	1.8	1.5	1.9	636	Main
TOT	15	1.7	1.6	1.8	547	Main
TOT	16	1.3	2.8	1.8	569	Main

14

## 15 **S.2. Mesh sensitivity analysis**

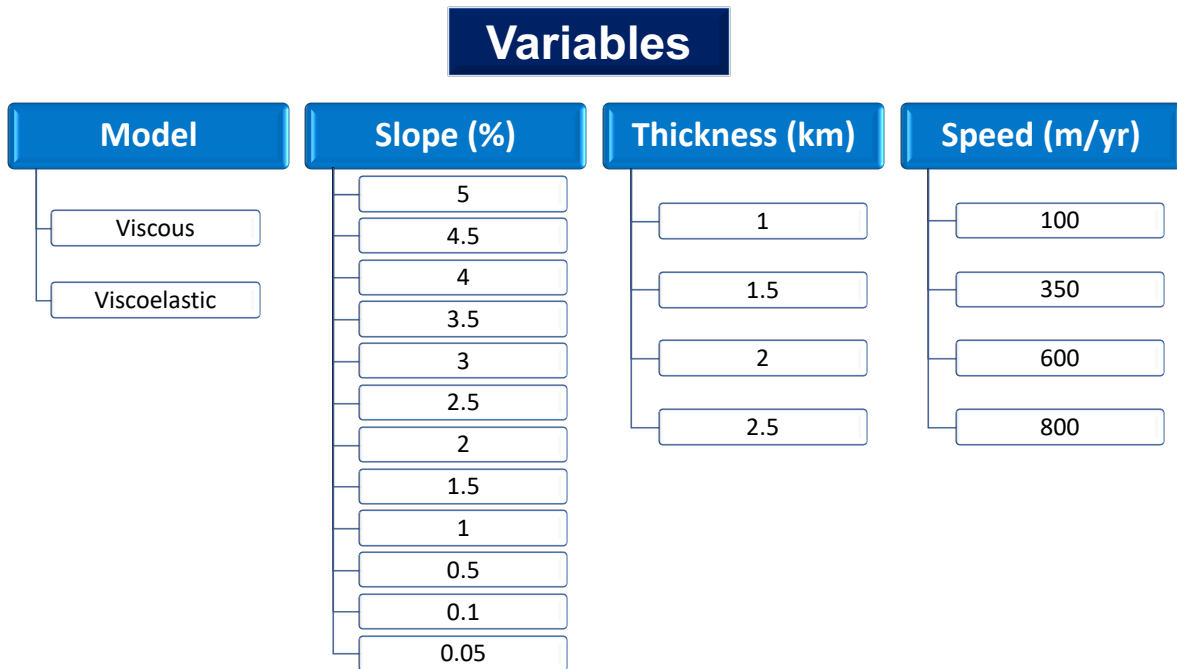
16 Models' sensitivity to mesh size was analyzed using 200 grounding zone width values (Figure S1), obtained for  
17 different mesh sizes of the lower domain surface (from 10 m to 250 m with 10 m step) and constant mesh size of  
18 250 m at the upper domain surface. For both models, the tests were performed for four sets of input parameters: 1) bed  
19 slope of 0.5 %, glacier thickness of 1 km, and ice inflow speed of 100 m/year (green dots in Figure S1); 2) bed slope  
20 of 5 %, glacier thickness of 1 km, and ice inflow speed of 100 m/year (red dots in Figure S1); 3) bed slope of 5 %, glacier  
21 thickness of 2.5 km, and ice inflow speed of 100 m/year (blue dots in Figure S1); 4) bed slope of 5 %, glacier  
22 thickness of 1 km, and ice inflow speed of 800 m/year (black dots in Figure S1).



23  
 24 **Figure S1.** Models mesh sensitivity check. Plots (a) and (c) correspond to the viscous model, and plots marked (b)  
 25 and (d) represent the viscoelastic model.

26 **S.3. DInSAR data-inferred parameters as model inputs**

27 Fixing 50 m and 250 m as mesh sizes at the lower and upper domain boundaries, respectively, and keeping the constant  
 28 glacier domain length of 20 km, each model was executed 192 times using all possible combinations of input  
 29 parameters, listed in Figure S2.



31 **Figure S2.** Schematic representation of the initial parameters. All possible combinations of these variables were  
 32 examined in the paper.

33 **S.4. Grounding zone evolution with glacier thickness**

34 The dependence of grounding zone width ( $GZ$ ) on glacier thickness ( $H$ ) for each inflow speed and bed slope,  
 35 approximated with a linear function  $GZ = a \cdot H + b$ , provides unique coefficients  $a$  and  $b$  for each model formulation,  
 36 bed slope, and ice inflow speed. These  $a$  and  $b$  values are listed in Table S2.

37 **Table S2.** Equations of the approximating lines of all considered dependences of the grounding zone magnitude  
 38 from the glacier thickness.

Slope, %	Inflow speed, m/year	Approximating line equation, viscous model	R <sup>2</sup> value, viscous model	Approximating line equation, viscoelastic model	R <sup>2</sup> value, viscoelastic model
5.0	100	$0.119 \cdot x + 1.209$	0.998	$0.081 \cdot x + 0.799$	1.000
	350	$0.071 \cdot x + 1.265$	0.975	$0.080 \cdot x + 0.779$	1.000
	600	$0.033 \cdot x + 1.297$	0.914	$0.072 \cdot x + 0.779$	0.987
	800	$0.027 \cdot x + 1.286$	0.985	$0.060 \cdot x + 0.776$	0.987
4.5	100	$0.119 \cdot x + 1.222$	0.999	$0.088 \cdot x + 0.904$	0.967
	350	$0.104 \cdot x + 1.216$	0.999	$0.076 \cdot x + 0.896$	0.969
	600	$0.083 \cdot x + 1.256$	1.000	$0.076 \cdot x + 0.868$	0.901
	800	$0.061 \cdot x + 1.303$	0.990	$0.064 \cdot x + 0.880$	0.874
4.0	100	$0.146 \cdot x + 1.316$	0.975	$0.120 \cdot x + 0.901$	1.000
	350	$0.126 \cdot x + 1.318$	0.987	$0.128 \cdot x + 0.860$	0.996
	600	$0.118 \cdot x + 1.294$	0.976	$0.112 \cdot x + 0.868$	0.942
	800	$0.111 \cdot x + 1.269$	0.985	$0.076 \cdot x + 0.908$	0.901
3.5	100	$0.225 \cdot x + 1.296$	0.989	$0.124 \cdot x + 1.001$	0.989
	350	$0.167 \cdot x + 1.369$	0.982	$0.132 \cdot x + 1.001$	0.983
	600	$0.090 \cdot x + 1.501$	0.939	$0.116 \cdot x + 0.977$	0.987
	800	$0.081 \cdot x + 1.527$	0.918	$0.108 \cdot x + 0.949$	0.975
3.0	100	$0.239 \cdot x + 1.415$	0.985	$0.152 \cdot x + 1.053$	0.997
	350	$0.205 \cdot x + 1.440$	0.976	$0.140 \cdot x + 1.081$	0.972
	600	$0.143 \cdot x + 1.545$	0.965	$0.144 \cdot x + 1.041$	0.973
	800	$0.099 \cdot x + 1.624$	0.975	$0.120 \cdot x + 1.073$	0.987
2.5	100	$0.227 \cdot x + 1.693$	0.969	$0.228 \cdot x + 1.049$	0.994
	350	$0.183 \cdot x + 1.731$	0.944	$0.188 \cdot x + 1.129$	0.991
	600	$0.194 \cdot x + 1.670$	0.958	$0.184 \cdot x + 1.121$	0.983
	800	$0.176 \cdot x + 1.685$	0.959	$0.150 \cdot x + 1.191$	0.977
2.0	100	$0.246 \cdot x + 1.925$	0.982	$0.276 \cdot x + 1.113$	0.994
	350	$0.221 \cdot x + 1.929$	0.975	$0.248 \cdot x + 1.276$	0.988
	600	$0.265 \cdot x + 1.839$	0.979	$0.244 \cdot x + 1.249$	0.982
	800	$0.216 \cdot x + 1.900$	0.968	$0.218 \cdot x + 1.235$	0.974
1.5	100	$0.370 \cdot x + 2.010$	0.970	$0.293 \cdot x + 1.372$	0.989
	350	$0.318 \cdot x + 2.113$	0.953	$0.309 \cdot x + 1.424$	0.985
	600	$0.350 \cdot x + 2.043$	0.975	$0.249 \cdot x + 1.568$	0.974
	800	$0.293 \cdot x + 2.165$	0.966	$0.249 \cdot x + 1.532$	0.993
1.0	100	$0.421 \cdot x + 2.628$	0.966	$0.492 \cdot x + 1.381$	0.999
	350	$0.333 \cdot x + 2.865$	0.986	$0.456 \cdot x + 1.618$	0.997
	600	$0.429 \cdot x + 2.565$	0.987	$0.380 \cdot x + 1.838$	0.991
	800	$0.391 \cdot x + 2.762$	0.994	$0.384 \cdot x + 1.778$	0.988
0.5	100	$1.002 \cdot x + 2.789$	0.911	$0.633 \cdot x + 1.705$	0.995

	350	$0.930 \cdot x + 3.055$	0.951	$0.709 \cdot x + 2.021$	0.989
	600	$0.906 \cdot x + 3.271$	0.912	$0.725 \cdot x + 2.181$	0.984
	800	$0.827 \cdot x + 3.549$	0.902	$0.685 \cdot x + 2.301$	0.975
0.1	100	$2.698 \cdot x + 2.020$	1.000	$1.021 \cdot x + 1.717$	0.999
	350	$2.731 \cdot x + 3.276$	0.997	$1.465 \cdot x + 1.950$	1.000
	600	$2.673 \cdot x + 4.187$	0.991	$1.565 \cdot x + 2.691$	0.999
	800	$2.583 \cdot x + 5.715$	0.969	$1.601 \cdot x + 2.827$	0.999
0.05	100	$3.41 \cdot x + 1.707$	1.000	$1.117 \cdot x + 1.838$	0.993
	350	$3.891 \cdot x + 2.764$	0.997	$1.690 \cdot x + 2.021$	0.999
	600	$3.983 \cdot x + 3.644$	0.987	$1.982 \cdot x + 2.518$	0.999
	800	$4.510 \cdot x + 4.792$	0.978	$2.026 \cdot x + 2.418$	0.998

39

### 40 S.5. Modifications in modeled grounding zones resulting from input parameters changes

41 Differences in grounding zone widths for the thickest and thinnest modeled glaciers for every inflow speed and every  
42 bedrock slope for both models are provided in Table S3.

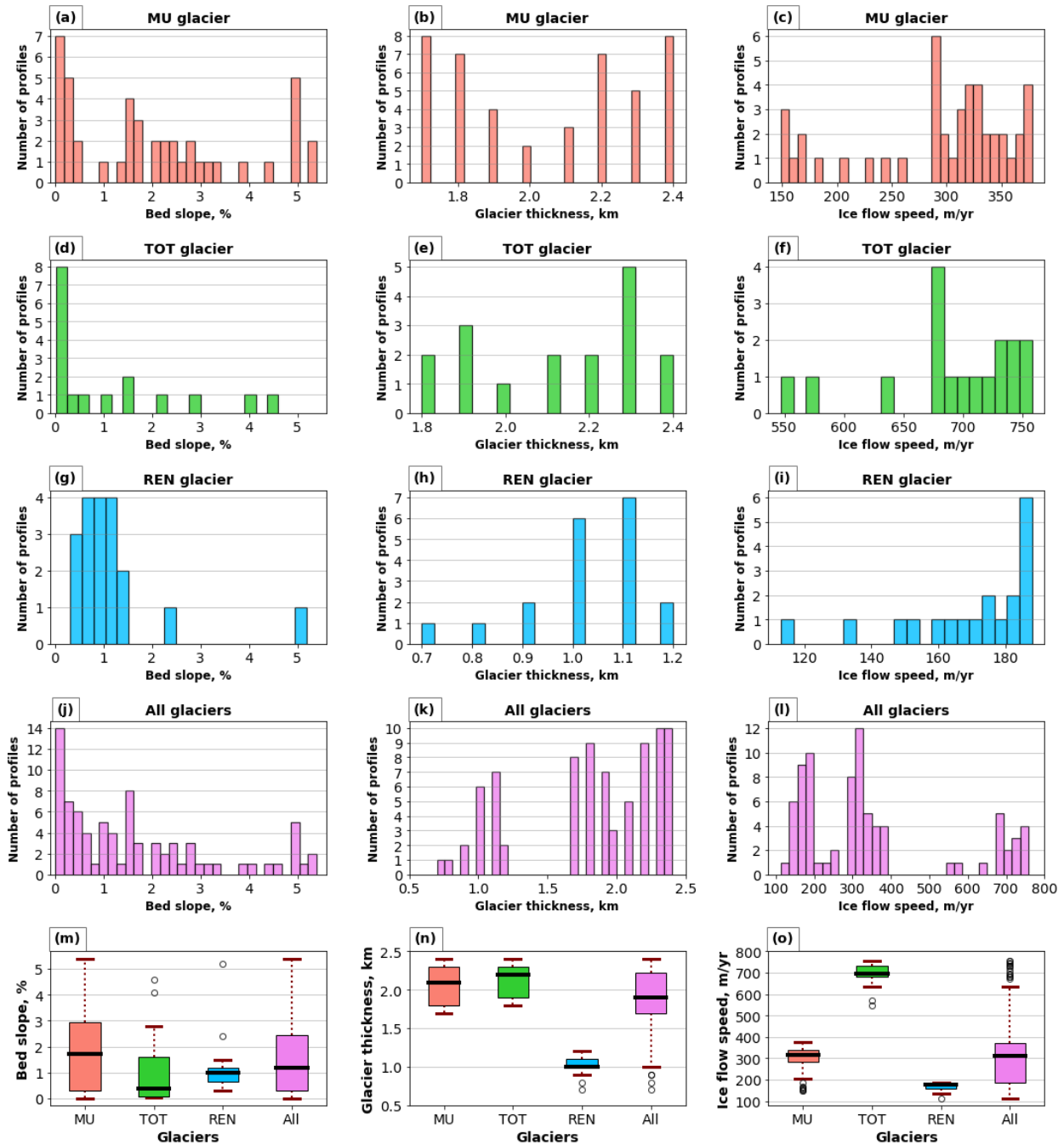
43 **Table S3.** Grounding zone width difference (in meters) for a 2500 m-thick glacier and a 1000 m-thick glacier.

$\Delta GZ = GZ_{H=2.5km} - GZ_{H=1.0km}, m$ (viscous model)												
Speed, m/yr	Bed slope, %											
	5.0	4.5	4.0	3.5	3.0	2.5	2.0	1.5	1.0	0.5	0.1	0.05
<b>100</b>	175	175	200	360	390	375	385	635	740	1866	4091	5066
<b>350</b>	120	160	170	265	350	320	370	550	545	1651	4266	6127
<b>600</b>	60	125	155	145	240	315	430	575	715	1696	4281	6627
<b>800</b>	35	85	150	145	135	270	370	510	615	1565	4412	6701
<b>Mean</b>	<b>98</b>	<b>136</b>	<b>169</b>	<b>229</b>	<b>279</b>	<b>320</b>	<b>389</b>	<b>568</b>	<b>654</b>	<b>1695</b>	<b>4263</b>	<b>6130</b>
$\Delta GZ = GZ_{H=2.5km} - GZ_{H=1.0km}, m$ (viscoelastic model)												
Speed, m/yr	Bed slope, %											
	5.0	4.5	4.0	3.5	3.0	2.5	2.0	1.5	1.0	0.5	0.1	0.05
<b>100</b>	121	141	180	200	240	360	440	481	761	961	1502	1521
<b>350</b>	120	121	201	220	240	300	400	501	720	1141	2222	2543
<b>600</b>	100	141	201	180	240	300	400	421	600	1202	2362	2963
<b>800</b>	80	121	141	180	200	260	370	401	620	1142	2482	3143
<b>Mean</b>	<b>105</b>	<b>131</b>	<b>181</b>	<b>195</b>	<b>230</b>	<b>305</b>	<b>403</b>	<b>451</b>	<b>675</b>	<b>1112</b>	<b>2142</b>	<b>2543</b>

44

### 45 S.6. Data-derived characteristics of the glaciers

46 The relative distributions of data-derived bed slopes, ice thicknesses, and ice floe speeds for the glaciers of interest  
47 are shown in Figure S3. The empty dots in the boxplots correspond to measurements determined by the IQR  
48 (Interquartile Range) method outliers. The IQR-based method identifies a data point as an outlier if it lays outside the  
49  $[Q_1 - 1.5 \cdot IQR; Q_3 + 1.5 \cdot IQR]$  range, where  $Q_1$  and  $Q_3$  are the 25<sup>th</sup> and the 75<sup>th</sup> percentile of a considered dataset.



50

51 **Figure S3.** Distributions of the ice-bed characteristics, measured along the selected profiles. Subplots (a)–(c)  
 52 correspond to Moscow University (MU) glacier; Subplots (d)–(f) correspond to Totten (TOT) glacier; Subplots  
 53 (g)–(i) correspond to Rennick (REN) glacier; Subplots (m)–(o) show the box plots for all three considered glaciers.  
 54 Left column of subplots shows the glacier distribution based on bed slope, middle column – distribution based on  
 55 glacier thickness, and right column – distribution based on ice flow speed.